Article ID: 1003 - 6326(2003)05 - 1208 - 05

Preliminary testing of $NiFe_2O_4$-NiO as ceramic matrix of cermet inert anode in aluminum electrolysis①

QIN Qing-wei(秦庆伟), LAI Yan-qing(赖延清), XIAO Jin(肖 劲),
LI Jie(李 [illegible]), LIU Ye-xiang(刘业翔)
(School of Metallurgical Science and Engineering, Central South University, Changsha 410083, China)

Abstract: Sintered samples of nickel ferrite-nickel oxide ceramic, usually used as the ceramic phase of cermet inert anode in aluminum electrolysis, were prepared and characterized. The solubilities of $NiFe_2O_4$-NiO ceramics were measured using an equilibration technique in the Na_3AlF_6-10% AlF_3-5% CaF_2-5 % Al_2O_3 melts at 960 ℃. Electrical resistivity was also measured for $NiFe_2O_4$-NiO ceramic samples prepared using the usual ceramic technique as function of temperature and content of NiO with an improved pyroconductivity test device, consisting of a specially constructed closed furnace and a Potentiostat/Galvanostat, based on the conventional direct current four-probe technique. Results show that, under the experimental conditions, the solubility of Fe from $NiFe_2O_4$ is 0.06% and Ni from $NiFe_2O_4$ is 0.008%. The solubility of Fe and Ni from $NiFe_2O_4$-NiO ceramic is inversely related to each other. The solubility of Ni increases but overall solubility of $NiFe_2O_4$-NiO ceramics decreases with increasing NiO content. The studied ceramic samples have a semiconductor behavior where electrical resistivity ρ decreases with increasing temperature and the resistivity ρ increases with increasing porosity. The resistivity ρ of $NiFe_2O_4$-NiO ceramic shows a minimum with increasing the content of NiO at various temperatures.

Key words: $NiFe_2O_4$-NiO ceramic; solubility; electrical resistivity; inert anode; aluminum electrolysis
CLC number: TF 111.52+2 **Document code:** A

1 INTRODUCTION

The idea of using inert anodes(also called non-consumable or oxygen-evolving anodes) in aluminum production is as old as the Hall-Héroult process, dating back to the discovery of one of the inventors, Hall[1]. Inert anodes are intended to replace the consumable carbon anode that is currently used. With a carbon anode, the cell reaction is

$$Al_2O_3 + 3/2C = 2Al + 3/2CO_2 \quad (1)$$

where a cryolite-based melt(Na_3AlF_6-AlF_3-CaF_2) at near 960 ℃ serves as solvent for the alumina. With an inert anode, the cell reaction will be

$$Al_2O_3 = 2Al + 3/2O_2 \quad (2)$$

The use of non-consumable anodes will eliminate the emissions of CO_2, CF_4(carbon fluoride) and PAH (polycyclic aromatic hydrocarbons) related to aluminum production using carbon anodes.

The principal requirements for inert anodes are low solubility in fluoride melts containing dissolved aluminum, high electronic conductivity, resistant to anode oxygen and little contamination of aluminum produced, ability to be fabricated in large shapes, stable electrical connection and adequate mechanical strength, relatively low cost and ready availability. Taken in sum, these requirements represent such a formidable that it is evident why the search for the inert anode has gone for so long.

Recent development efforts concentrate on metal, cermet, and ceramic inert anodes. Cermets are attractive as they combine the advantage of two classes of materials, namely, metals(desirable for their high electrical conductivity) and ceramics (desirable for their chemical inertness). The questions of thermal shock resistance and reliable electrical contact to the busbar have potential settle possibility. Much research work shows that complex oxides, in particular, nickel ferrite spinel has great utilization in cermet inert anodes matrix due to its high thermodynamic stability and favorable electro-catalytic activity for oxygen evolution. However, the high electrical resistance of this material and the high solubility of Fe are intolerable[2-12].

In this work, ceramic samples consisting of nickel ferrite and nickel oxide as inert anodes matrix are prepared with a conventional ceramic process. Solubility of oxides for inert anodes in cryolite-based melts is tested using an equilibration technique. An improved pyroconductivity test device was constructed based on the conventional direct current four-probe technique. The electrical resistivity as a function of temperature and NiO content for various $NiFe_2O_4$-NiO ceramic samples is investigated in the temperature range from 300 ℃ to 1 000 ℃ in air. And main

① **Foundation item:** Project(G1999064903) supported by the National Key Fundamental Research and Development Program of China
Received date: 2002 - 11 - 19; **Accepted date:** 2003 - 03 - 21
Correspondence: QIN Qing-wei, PhD; + 86-731-8830474; E-mail: qingweiqin@yahoo.com.cn

results are introduced.

2 EXPERIMENTAL

2.1 Preparation of $NiFe_2O_4$-NiO ceramic

The $NiFe_2O_4$-NiO ceramic raw material powder was prepared from analytical grade chemicals. Nickel mono-oxide and iron oxide were milled with ball mill, and screened through a 200-mesh screen, respectively. Then the raw material powder was dried, blended according to ceramic compositions, and calcined in air. Batch calcinations were conducted at 1 150 ℃ for 6 h to react the raw materials and create the NiO and $NiFe_2O_4$ presenting in the resulting powder. The target powder was evaluated for chemical purity, particle size distribution and surface area. X-ray diffraction (XRD) showed no traces of uncalcined powder or foreign phases.

The presintered oxides were ground finely, and then pressed in the form of cylinder at constant pressure of 200 MPa without using any binder. Finally, the samples were sintered at 1 250 ℃ and 1 400 ℃ for 4 h in the presence of air. Green compaction of short samples (diameter of 20 mm and height of 10 mm) were used for solubility tests in cryolite-alumina melts and longer samples (diameter of 20 mm and height of 40 mm) were used for electrical resistivity tests. Green density of 60%－70% of theoretical was obtained.

Final sintered density, porosity and expansion characteristics were determined by ASTM Archimetedes method C373-88(1999) prior to solubility and electrical resistivity tests.

2.2 Solubility measurement

Ceramic solubility measurements were conducted using an equilibration technique. The experimental apparatus is shown in Fig. 1. Approximately 100 g melt was contained in an 80 mL platinum crucible. To prevent vaporization of AlF_3 in the furnace, the platinum crucible was sealed in an alumina crucible, which in turn was supported on a sintered corundum plate covered with some powder alumina. The entire assembly was inserted in a upright resistance furnace.

Cylinders of the $NiFe_2O_4$-NiO ceramic were equilibrated with the melt. The solubility of ceramics was determined from the contamination of the electrolyte. Samples of the electrolyte were taken before the immersion of the anode and every 1 h during the test. When sampling, the corundum crucible was moved. The samples were frozen on a platinum rod which was quickly dipped into the electrolyte and removed for solidification. The samples were ground in an agate mortar and dissolved in concentrated $HClO_4$ in order to be analyzed by atomic absorption spectrum. The precision of the analyses is approximately ±5%.

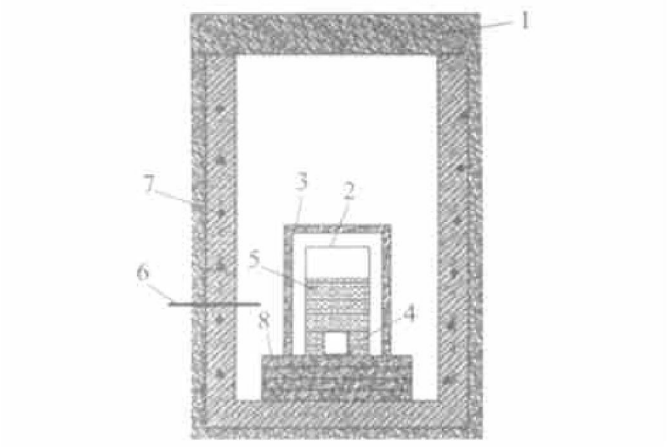

Fig. 1 Experimental apparatus for solubility measurement
1—Sintered alumina lid; 2—Platinum crucible; 3—Corundum crucible; 4—Sample; 5—Electrolyte melt; 6—Thermocouple, type S, with corundum sheath; 7—Heating element; 8—Sintered corundum plate

2.3 Electrical resistivity measurement

As shown in Fig. 2, an improved pyroconductivity test device, consisting of a specially constructed closed furnace and a potentiostat, was constructed based on the conventional direct cur-

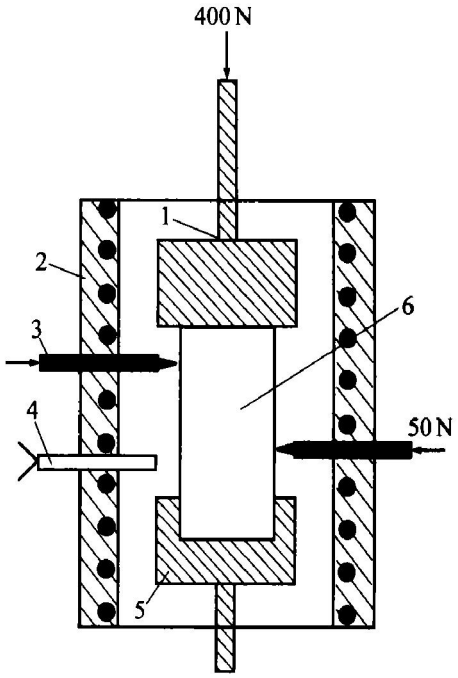

Fig. 2 Experimental apparatus for electrical resistivity measurement at high temperature
1—Top molybdenum clamp for current conduct; 2—Heating furnace; 3—Potential probes; 4—Thermocouple, type S, with corundum sheath; 5—Bottom molybdenum clamp for current conduct; 6—Specimen

rent four-probe technique. Symmetrical current distribution in the specimen was obtained by keeping a fixed pressure of 400 N and good contact between the specimen and clamps at any temperature. The samples were polished well to have smooth parallel surfaces. A Model 273A Potentiostat/Galvanostat was used to supply direct current and continuously monitor to the current intensity and voltage between two potential probes, which can be adjusted outside the heating furnace to well contact with the specimen by keeping a fixed pressure of 50 N. Test results of pure copper and spectrographic graphite specimens showed that the reliability and reproducibility are excellent. The electrical conductivity ρ as a function of temperature for various $NiFe_2O_4$-NiO ceramics was investigated at the temperature ranging from 300 ℃ to 1 000 ℃ to study the influential factors, which included the particle size of raw materials, manufacture process, phase composition and morphology etc.

3 RESULTS AND DISCUSSION

3.1 Effect of NiO content on solubility of $NiFe_2O_4$-NiO ceramics

Fig. 3 shows the approach to equilibrium for $NiFe_2O_4$ ceramic. Steady-state concentrations, which were taken to be the solubilities, reached approximately 6 – 8 h after the oxide cylinders were dropped into the NaF-AlF_3-CaF_2-Al_2O_3 melts. The melt was allowed to equilibrate for about 8 h at each temperature.

Fig. 4 shows the solubility of $NiFe_2O_4$-NiO ceramics plotted as a function of NiO content. The Fe content in the electrolyte melts decreases with increasing NiO content in ceramics, while the Ni concentration in the electrolyte melts increases with increasing NiO content in ceramics. Thus, nickel ferrite-based inert anodes should be formulated with excess NiO to decrease the concentration of Fe in electrolyte melts and the corrosion rate of inert anodes in melts.

The solubilities of Fe and Ni from $NiFe_2O_4$ are inversely related to each other as follows (for stoichiometric $NiFe_2O_4$)[13]:

$$K = 1/[(X_{Fe_2O_3} \cdot X_{NiO}) \cdot (\gamma_{Fe_2O_3} \cdot \gamma_{NiO})] \quad (3)$$

3.2 Effect of temperature on electrical resistivity of $NiFe_2O_4$-NiO ceramics

Table 1 shows the DC electrical resistivity ρ of several $NiFe_2O_4$-NiO samples in air, as a function of temperature. The electrical resistivity of these ceramics is rather high, about 0.75–4.3 Ω·cm even at 1 000 ℃, compared to that below 0.005 Ω·cm for carbon anodes, presently used. The use of this material will not be economical because of a large IR drop in the anode even considering the fact that an inert anode may be designed to provide a large ratio of the anode area to the anode length, compared with carbon anodes. Thus, $NiFe_2O_4$-NiO ceramic should be doped with metals or other oxides to decrease its electrical resistivity.

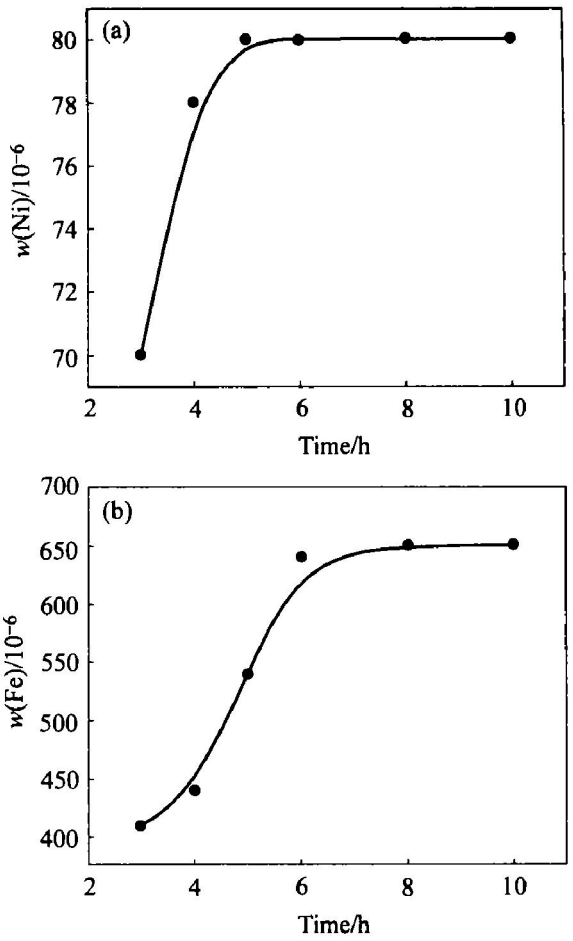

Fig. 3 Bath analyses results illustrating time needed for equilibration of $NiFe_2O_4$ in melt (mole ratio of NaF/AlF_3= 2.3, $w(CaF_2)\%$= 5, $w(Al_2O_3)\%$= 5) at 960 ℃

In Fig. 5, the natural logarithm of DC electrical resistivity, $\ln\rho$ is plotted as a function of 1 000 T^{-1} and it can be seen that $\ln\rho$ vs 1 000 T^{-1} shows a straight line as expected for a semiconductor material in two temperature ranges, respectively. The reasons for it are not clear. One possible cause is that a change in the gradient of the straight line may take place on passing through the Curie point as reported[14]. In fact[15, 16], this decrease of ρ with increasing temperature is normal for semiconductors which is controlled by the Arrhenius relation expressed as Eqn. (4):

$$\rho = \rho_0 \exp[E/kT] \quad (4)$$

where ρ_0 is the pre-exponential constant or resistivity at infinitely high temperatures. E is the activation energy for electric conduction and k is the Boltzmann constant.

NiO absorbs oxygen and decreases in ρ with increasing the temperature, electron hopping be-

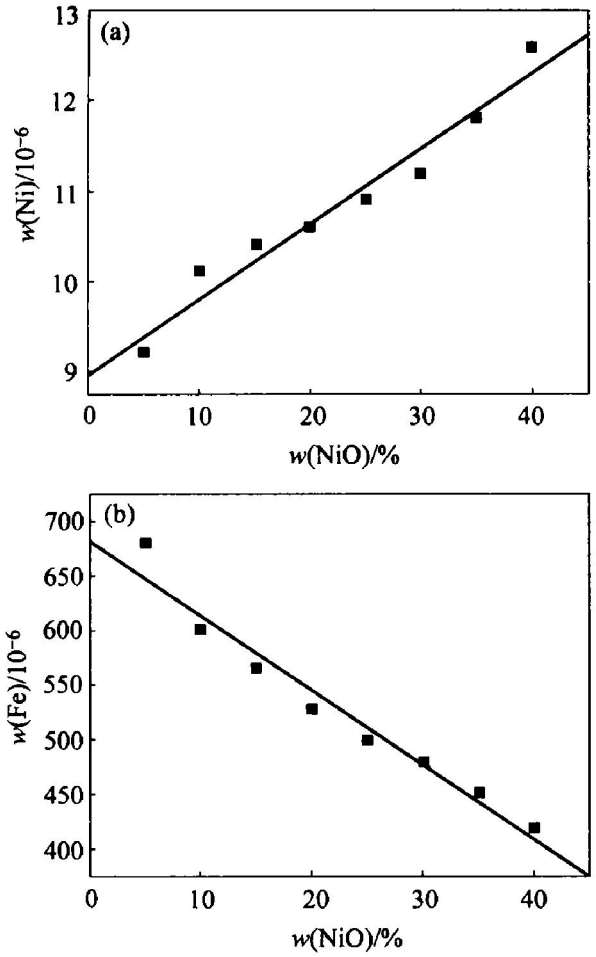

Fig. 4 Effect of NiO content on solubility of $NiFe_2O_4$-NiO ceramics in melts(mole ratio of NaF/AlF_3= 2.3, $w(CaF_2)\%$= 5, $w(Al_2O_3)\%$= 5) at 960 ℃ for 8 h

tween Ni^{2+} and Ni^{3+} as expressed in Eqns. (5), (6).

$$Ni^{2+} \Leftrightarrow Ni^{3+} + e \quad (5)$$

$$Ni^{3+} \Leftrightarrow Ni^{2+} + p \quad (6)$$

For nickel ferrite, the presence of Ni ions on octahedral-(B) sites, and Fe ions on tetrahedral-(A) sites and B-sites favor the ion exchange interactions expressed as Eqn. (7):

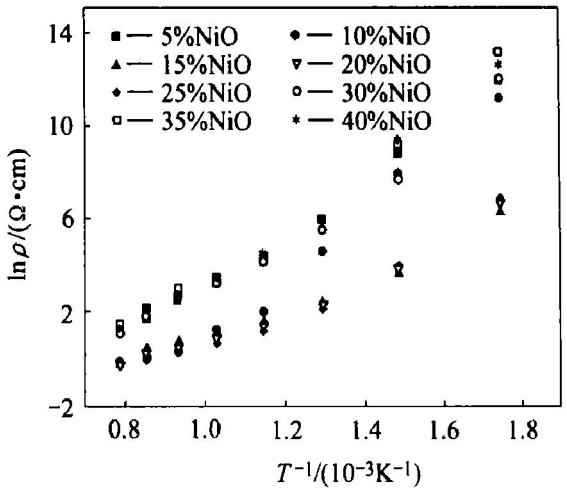

Fig. 5 Relation between temperature and electrical resistivity ρ of NiO-$NiFe_2O_4$ ceramics

$$Ni^{2+} + Fe^{3+} \Leftrightarrow Ni^{3+} + Fe^{2+} \quad (7)$$

Thus the conduction mechanism for the n-type semiconductor is predominantly due to the hopping of electrons from Fe^{2+} to Fe^{3+} ions while that for the p-type semiconductor is due to the holes transfer from Ni^{3+} to Ni^{2+} ions. It seems that the present samples have both types of charge carriers, which participate in the conduction process, and the conductivity is the sum of both types.

3.3 Effect of NiO content on electrical resistivity and other properties of $NiFe_2O_4$-NiO ceramics

The relationships of NiO content and the properties of $NiFeO_4$-NiO ceramics are listed in Tables 1, 2 and 3, respectively. From Table 1, one can see that the resistivity ρ at various temperatures of $NiFe_2O_4$-NiO ceramics has a minimum with increasing the content of NiO. The electrical resistivity of $NiFe_2O_4$-NiO ceramics containing 25% NiO is the lowest at temperature of 500~1 000 ℃.

The reasons for above phenomenan are not very clear. But one might suggest two common causes: the first one is the electrical characteristics

Table 1 Electrical resistivity of NiO-$NiFe_2O_4$ ceramics at various temperatures(Ω·cm)

Temperature/ ℃	5% NiO+ $NiFe_2O_4$	10% NiO+ $NiFe_2O_4$	15% NiO+ $NiFe_2O_4$	20% NiO+ $NiFe_2O_4$	25% NiO+ $NiFe_2O_4$	30% NiO+ $NiFe_2O_4$	35% NiO+ $NiFe_2O_4$	40% NiO+ $NiFe_2O_4$
300	147 717.00	69 310.00	529.18	755.06	918.40	147 329.00	498 855.00	287 993.00
400	6 065.80	2 646.10	36.08	44.54	48.62	2 110.30	8 938.00	10 781.00
500	373.01	95.95	10.56	9.50	8.09	235.26	374.60	372.19
600	64.80	6.99	5.01	3.92	3.12	63.35	80.60	87.69
700	25.96	3.29	2.87	2.31	1.87	25.01	30.50	31.66
800	12.23	1.40	2.02	1.61	1.32	14.57	18.95	13.66
900	5.53	1.06	1.47	1.18	0.98	5.92	7.98	8.22
1 000	2.93	0.85	0.82	0.79	0.75	2.91	3.59	4.27

Table 2 Bulk density, relative density and porosity versus NiO content of $NiO-NiFe_2O_4$ ceramic sintered at 1 400 ℃ for 4 h

w(NiO)/%	Theoretical density/(g·cm^{-3})	Relative density/%	Porosity/%
5	5.43	92.36	7.64
10	5.49	90.22	9.78
15	5.55	88.27	11.74
20	5.61	86.15	13.85
25	5.67	84.15	15.85
30	5.73	82.02	17.98
35	5.80	79.87	20.13
40	5.87	77.87	22.13

Table 3 Effect of porosity(θ) on electrical resistivity of $NiFe_2O_4$-20% NiO ceramic(Ω· cm)

Temperature/℃	θ= 27.12%	θ= 13.85%
300	281 282.00	755.00
400	5 437	44.54
500	395.60	9.20
600	96.27	3.92
700	30.88	2.31
800	12.23	1.62
900	7.40	1.18
1 000	3.11	0.79

or crystal structure characteristics of NiO and $NiFe_2O_4$, and the second one is the sintering performance of NiO and $NiFe_2O_4$, which can be reflected with the relative density and porosity of the sintered $NiFe_2O_4$-NiO ceramics.

If just considering the first cause, i.e. all $NiFe_2O_4$-NiO ceramics possess the same porosity and relative density, the electrical resistivity should decrease with increasing NiO content. However, from Table 2, the relative density of $NiFe_2O_4$-NiO ceramics decreases and its porosity increases with increasing the NiO content. The relative density and porosity are 92.36% and 7.64% for $NiFe_2O_4$-NiO ceramic containing 5% NiO, but 77.87% and 22.13% for $NiFe_2O_4$-NiO ceramic containing 40% NiO, respectively. When the porosity increases, the number of pores, vacancies and scattering centers for the electric charge carriers increase. As a result, a marked increase in the values of the electrical resistivity will be produced. So the electrical resistivity should increase with increasing NiO content considering the second cause. And from Table 3, the electrical resistivity ρ of $NiFe_2O_4$-NiO ceramics containing 20% NiO, at 300 – 1 000 ℃, increases increasing markedly with the porosity θ by raising the sintering temperature from 1 250 ℃ to 1 400 ℃.

REFERENCES

[1] Hall C M. Process of reducing aluminium from its fluoride salts by electrolysis[P]. US 400664, 1886 – 9.

[2] The Aluminum Association. Aluminum Industry Technology Roadmap[EB/OL]. http://www.oit.doe.gov/aluminum/pdfs/tech road.pdf.

[3] The Aluminum Association and the US Department of Energy. Inert Anode Roadmap: a Framework for Technology Development[EB/OL]. http://www.oit.doe.gov/aluminum/pdfs/inevt road.pdf.

[4] Hanneman R E, Hayden H W, Goodnow W, et al. Report of the American society of mechanical engineers' technical working group on inert anode technologies[EB/OL]. http://www.oit.doe.gov/aluminum/tools.shtml.

[5] de Nora V. Aluminium electrowinning—the future[J]. Alumnium, 2000, 76(12): 998 – 999.

[6] Welch B J, Hyland M M, James B J. Future materials requirements for the high-energy-intensity production of aluminum[J]. JOM, 2001, 53(2): 13 – 18.

[7] Sadoway D R. Inert anode for the Hall-Héroult cell: The ultimate materials challenge[J]. JOM, 2001, 53(5): 34 – 35.

[8] Ray S P. Effect of operating parameters on performance of inert anodes in Hall-Heroult cells[J]. Light Metals: 367 – 380.

[9] Thonstad J, Olsen E. Cell Operation and Metal Purity Challenges for the Use of Inert Anodes[J]. JOM, 2001, 53(2): 36 – 38.

[10] Belyaev A I, Studentsov A E. Electrolysis of alumina with non-combustible (metallic) anodes[J]. Legkie Metally, 1937, 6(3): 17 – 22.

[11] Ray S P. Inert anodes for hall cells[J]. Light Metals, 287 – 298.

[12] Pawlek R P. Inert anodes: an update[J]. Light Metals, 449 – 456.

[13] DeYoung D H. Solubility of oxides for inert anodes in cryolite-based melts[J]. Light Metals, 299 – 307.

[14] Elshora A I, Elhiti M A, Elnimr M K, et al. Semiconductivity in $Ni_{1+x}Mn_xFe_{2-2x}O_4$ ferrites[J]. Journal of Magnetism and Magnetic Materials, 1999, 204(1 – 2): 20 – 28.

[15] Abdeen A M. Electric conduction in Ni-Zn ferrites[J]. Journal of Magnetism and Magnetic Materials, 1998, 185(2): 199 – 206.

[16] Elshabasy M. DC electrical properties of Zn-Ni ferrites [J]. Journal of Magnetism and Magnetic Materials, 1997, 172(1 – 2): 188 – 192.

(Edited by LI Xiang-qun)